

## A DENSE GAS TRIGGER FOR OH MEGAMASERS

JEREMY DARLING<sup>1</sup>

*Draft version October 29, 2018*

### ABSTRACT

HCN and CO line diagnostics provide new insight into the OH megamaser (OHM) phenomenon, suggesting a dense gas trigger for OHMs. We identify three physical properties that differentiate OHM hosts from other starburst galaxies: (1) OHMs have the highest mean molecular gas densities among starburst galaxies; nearly all OHM hosts have  $\bar{n}(\text{H}_2) = 10^3\text{--}10^4\text{ cm}^{-3}$  (OH line-emitting clouds likely have  $n(\text{H}_2) > 10^4\text{ cm}^{-3}$ ). (2) OHM hosts are a distinct population in the nonlinear part of the IR-CO relation. (3) OHM hosts have exceptionally high dense molecular gas fractions,  $L_{\text{HCN}}/L_{\text{CO}} > 0.07$ , and comprise roughly half of this unusual population. OH absorbers and kilomasers generally follow the linear IR-CO relation and are uniformly distributed in dense gas fraction and  $L_{\text{HCN}}$ , demonstrating that OHMs are independent of OH abundance. The fraction of non-OHMs with high mean densities and high dense gas fractions constrains beaming to be a minor effect: OHM emission solid angle must exceed  $2\pi$  steradians. Contrary to conventional wisdom, IR luminosity does not dictate OHM formation; both star formation and OHM activity are consequences of tidal density enhancements accompanying galaxy interactions. The OHM fraction in starbursts is likely due to the fraction of mergers experiencing a temporal spike in tidally driven density enhancement. OHMs are thus signposts marking the most intense, compact, and unusual modes of star formation in the local universe. Future high redshift OHM surveys can now be interpreted in a star formation and galaxy evolution context, indicating both the merging rate of galaxies and the burst contribution to star formation.

*Subject headings:* masers — galaxies: interactions — galaxies: nuclei — galaxies: starburst — radio lines: galaxies

### 1. INTRODUCTION

OH megamasers (OHMs) are rare luminous 18 cm masers associated with major galaxy merger-induced starbursts. The hosts of OHMs are (ultra)luminous IR galaxies ([U]LIRGs), and the OHM fraction in (U)LIRGs peaks at about 1/3 in the highest luminosity mergers (Darling & Giovanelli 2002a). It is not known whether all major mergers experience an OHM stage or what detailed physical conditions produce OHMs, but it is clear that OHMs are a radically different phenomenon from the aggregate OH maser emission associated with “normal” (Galactic) modes of star formation in galaxies. Lo (2005) posed a key question: why do 80% of LIRGs show no OHM activity? To reframe the question: given two merging systems with similar global IR and radio continuum properties in the same morphological stage of merging, why does one show OHM emission while the other does not? What is the difference between the two systems? Perhaps there is no difference and the fraction of OHMs among mergers simply reflects beaming or OH abundance. Or perhaps OHM activity depends on small-scale conditions that are decoupled from global properties of mergers.

The provenance of OHM emission vis-à-vis the host galaxy has been extensively investigated in the radio through X-ray bands by comparing samples of OHM galaxies to similarly selected non-masing control samples. For example, Darling & Giovanelli (2002a) and Baan & Klöckner (2006) studied radio and IR properties vis-à-vis the AGN versus starburst contributions to OHM activity, Baan *et al.* (1992) and Darling & Giovanelli (2002a) investigated the OHM fraction in (U)LIRGs versus star formation rate and IR color,

Baan, Salzer, & LeWinter (1998) and Darling & Giovanelli (2006) used optical spectral classification to distinguish populations and to quantify AGN fraction in OHM hosts, and Vignali *et al.* (2005) conducted an X-ray study of the contribution of AGNs to OHM hosts. While some of these studies pointed to minor differences in statistical samples of OHM hosts versus nonmasing systems, they could not identify on a case-by-case basis which systems would harbor OHMs and which would not based on any observable quantity except the OH line itself.

Theoretical modeling of OHM formation has seen a recent renaissance: Parra *et al.* (2005) model the  $\sim 50$  pc molecular torus in III Zw 35 and show how OHM emission is a stochastic amplification of unsaturated emission by multiple overlapping clouds, and Lockett & Elitzur (2007) show how the general excitation of OHMs is fundamentally different from Galactic OH maser emission and predict that a single excitation temperature governs all 18 cm OH lines. While the physics of OHMs is crystallizing, and models predict that beaming is not likely to be the dominant factor in the OHM fraction among (U)LIRGs, it remains unclear on a case-by-case basis what conditions found in starbursts drive or prohibit OHM formation.

Here we describe a dense gas trigger for OHM formation, at last identifying physical observable properties that differentiate OHMs from nonmasing mergers. We identify OHMs, OH absorbers, OH kilomasers, and OH non-detections in the Gao & Solomon (2004a; hereafter GS04a) sample (§2) and employ CO(1–0) and HCN(1–0) molecular gas tracers to show that while OH absorbers appear nearly uniformly distributed in  $L_{\text{IR}}$  and  $L_{\text{HCN}}$ , OHMs represent the *majority* of the nonlinear population in the IR-CO relation (§3). In combination with a Kennicutt-Schmidt-based star formation model of CO line emission by Krumholz & Thompson (2007), we

<sup>1</sup> Center for Astrophysics and Space Astronomy, Department of Astrophysical and Planetary Sciences, University of Colorado, 389 UCB, Boulder, CO 80309-0389; jdarling@origins.colorado.edu

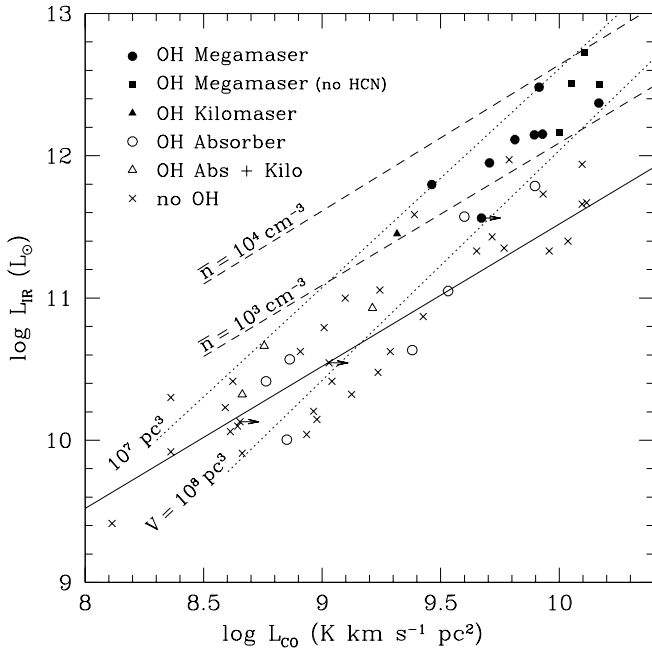


FIG. 1.— IR luminosity versus CO line luminosity in HCN-detected galaxies with known OH properties from the GS04a sample. The legend indicates symbols for OH megamasers, OH kilomasers, OH absorbers, and objects with no detected OH lines. The solid line is a linear fit by Gao & Solomon (2004b) to galaxies with  $L_{\text{IR}} < 10^{11} L_{\odot}$  ( $L_{\text{IR}} = 33 L_{\text{CO}}$  in units above), the dotted lines indicate a constant total volume of molecular material, and the dashed lines indicate the mean  $\text{H}_2$  density derived from Krumholz & Thompson (2007).

identify a high mean molecular density driving OHM emission, and from the HCN/CO ratio we find that OHM galaxies are exclusively high dense gas fraction starbursts (§3). Now that we can at last observe quantities that are highly predictive of OHM activity, we can employ OHMs at high redshifts as probes of major galaxy mergers and extreme star formation (§4).

## 2. THE SAMPLE

The somewhat diverse GS04a HCN sample that forms the basis for this study includes most IR- and CO-bright galaxies (by flux) and most local northern ULIRGs ( $cz < 20,000 \text{ km s}^{-1}$ ). Table 1 lists basic properties and line luminosities of all galaxies in the sample that have been observed in the 1667 MHz OH line by various groups. The HCN sample includes 8 OHMs, 12 OH absorption systems, 4 OH kilomasers, and 40 OH nondetections. While the division between OH kilomasers and OHMs at  $L_{\text{OH}} = 10 L_{\odot}$  is rather arbitrary, the  $L_{\text{OH}}$  values for the OH kilomasers are well separated from the OHMs in Table 1 by 2 orders of magnitude. Three of the four OH kilomasers in this sample show both emission and absorption. OH types marked with an asterisk are somewhat uncertain and have been omitted from all subsequent analysis and figures. We have included in Figure 1 four additional OHMs that have been detected in CO by Solomon *et al.* (1997) but have not yet been observed in HCN: IRAS 03521+0028, 14070+0525, 16090–0139, and 18368+3549.

## 3. RESULTS

Sorting the GS04a sample by OH type — megamaser, kilomaser, absorber, or non-detection — reveals striking properties of OHM host galaxies that set them apart from other

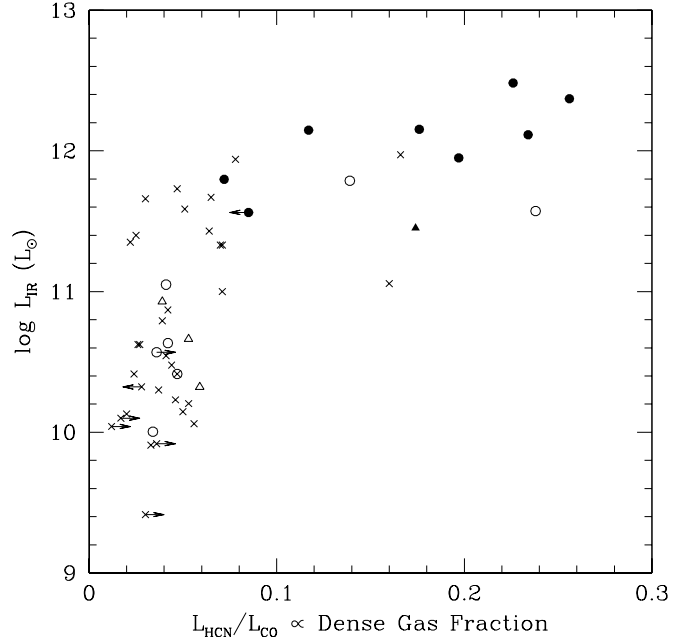


FIG. 2.— IR luminosity versus  $L_{\text{HCN}}/L_{\text{CO}}$ , a proxy for the dense gas fraction, in HCN-detected galaxies with known OH properties from the GS04a sample. Symbols are identical to those used in Figure 1.

starburst galaxies. Figure 1 shows that OHMs comprise the majority of the population that is offset from the linear  $L_{\text{IR}}-L_{\text{CO}}$  relation. OH absorbers and kilomasers, however, generally follow the linear IR-CO relation. Using the relationship between  $L_{\text{IR}}/L_{\text{CO}}$  and the mean  $\text{H}_2$  density,  $\bar{n}$ , derived from Kennicutt-Schmidt laws by Krumholz & Thompson (2007, Fig. 2), we show in Figure 1 that all OHMs in the sample are produced in starburst volumes of  $10^7-10^8 \text{ pc}^3$  (radii  $\sim 130-290 \text{ pc}$ ) and that all but one OHM have extremely high volume-averaged molecular densities,  $\bar{n} = 10^3-10^4 \text{ cm}^{-3}$ . In fact, 7 of 10 objects in the HCN sample in this density range are OHMs and one is a nonabsorbing OH kilomaser. Note that  $\bar{n}$  is the *mean*  $\text{H}_2$  density; the clouds responsible for OHMs within these regions must be significantly denser than the mean. There are many nonmasing systems with high  $L_{\text{IR}}$  at lower densities and larger volumes than the OHMs, demonstrating that molecular density, not the IR radiation field, is the OHM trigger.

Equally striking is the segregation of OHMs from nonmasing starbursts in a plot of  $L_{\text{IR}}$  versus  $L_{\text{HCN}}/L_{\text{CO}}$ , a proxy for dense molecular gas fraction (Gao & Solomon 2004b). Figures 2 and 3 show that all 8 OHMs (and the nonabsorbing OH kilomaser) have  $L_{\text{HCN}}/L_{\text{CO}} > 0.07$ . There are also 2 OH absorbers and 5 OH nondetections in this regime, so OHMs comprise roughly half of this unusual population. There are no OHMs with  $L_{\text{HCN}}/L_{\text{CO}} < 0.07$ , but there are many other luminous systems, including OH absorption systems and OH absorbers with coincident kilomaser emission. Galaxies with OH absorption are fairly uniformly distributed in  $L_{\text{IR}}$  and dense gas fraction, indicating that OH abundance is not a factor in OHM formation. The  $\gtrsim 50\%$  fraction of OHMs in dense starbursts constrains OHM beaming to be a minor contributor to the OHM fraction in LIRGs, and we conclude that the OHM emission solid angle must be greater than  $2\pi$  steradians.

## 4. DISCUSSION

A dense gas trigger for OHM formation is consistent with the modeling work by Parra *et al.* (2005) showing that the critical component for OHM formation is cloud-cloud overlap; a starburst-scale high mean molecular density and high dense gas fraction both provide the required overlap of many dense clouds. What is not yet clear is whether OHM activity is a density effect or simply a concentration effect. The rough size scales bracketing all OHMs in Figure 1 are also consistent with the 100–200 pc OHM emission regions observed with VLBI (e.g., Pihlström *et al.* 2001; Rovilos *et al.* 2003).

It is somewhat surprising that significant differences between OHM hosts and nonmasing systems are seen at all in unresolved observations because masing nuclei are “contaminated” by nonmasing nuclei within mergers. We expect that the observed differences between OHMs and nonmasing starbursts would intensify in resolved observations. However, high dipole moment molecules such as HCN and CS may be good OHM location-selective tracers that obviate the need to obtain subarcsecond resolution.

It is certain that the OHM phase is transitory because star formation rates found in these systems are sustainable for  $10^7$ – $10^8$  yr, whereas the complete merging process requires of order  $10^9$  yr. What is not known, however, is whether this mode of star formation is a universal, inevitable stage or an uncommon event in major galaxy mergers. Tidal torques spike multiple times during mergers, and many major mergers are likely to experience a ULIRG phase, but will most mergers experience the even more extreme OHM phase? The simple observation that about 20% of LIRGs with  $L_{\text{FIR}} > 10^{11.2} L_{\odot}$  show OHM activity (Darling & Giovanelli 2002a) suggests that if *all* LIRGs experience an OHM stage, then the OHM lifetime is of order 20% of the LIRG lifetime. If only a subset of LIRGs have an OHM stage, then the OHM lifetime must be longer. It is also possible that OHMs draw from a larger “pool” of galaxies that begin at lower  $L_{\text{FIR}}$  than the LIRG sample, which would allow a shorter OHM lifetime. Constraints on the OHM lifetime are clearly critical to understanding OHMs and the modes of star formation in major

galaxy mergers.

## 5. CONCLUSIONS

We have identified three closely related physical properties that differentiate OHMs from other starburst galaxies: OHM hosts have the highest mean molecular gas densities, they are a distinct population in the nonlinear part of the IR-CO relation, and they reside in galaxies with exceptionally high dense molecular gas fractions. We conclude that molecular gas must be concentrated and massive in order to reach the mean density required to form an OHM in a galactic nucleus. IR luminosity is not a condition for OHM formation; both star formation and OHM activity are consequences of the tidal density enhancements accompanying galaxy interactions. The fraction of OHMs in dense starbursts constrains OHM beaming to be a minor effect: OHM solid angle emission must be greater than  $2\pi$  steradians. These conclusions are in good agreement with the stochastic cloud-cloud overlap amplification model by Parra *et al.* (2005). The rather uniform distribution of OH absorbers in IR, HCN, and CO luminosity suggests that OH abundance is not a significant factor in OHM formation. The main caveat to these conclusions is that the sample of OHMs with HCN observations remains small, and should be expanded, particularly to higher redshifts to include “typical” OHMs.

OHMs are signposts of the most intense, compact, and unusual modes of star formation in the local universe, and surveys for OHMs will now provide detailed information about the detected host galaxies and their mode of star formation. The missing datum required for a complete interpretation of OHM surveys, however, is the OHM lifetime.

This work benefited significantly from comments by the anonymous referee. This research has made use of the NASA/IPAC Extragalactic Database (NED), which is operated by the Jet Propulsion Laboratory, California Institute of Technology, under contract with NASA.

## REFERENCES

- Baan, W. A., Haschick, A. D., Buckley, D. & Schmelz, J. T. 1985, *ApJ*, 293, 394  
 Baan, W. A., Haschick, A. D., & Schmelz, J. T. 1985, *ApJ*, 298, L51  
 Baan, W. A., Haschick, A. D., & Henkel, C. 1989, *ApJ*, 346, 680  
 Baan, W. A. 1989, *ApJ*, 338, 804  
 Baan, W. A., Haschick, A., & Henkel, C. 1992, *AJ*, 103, 728  
 Baan, W. A., Salzer, J. J., & LeWinter, R. D. 1998, *ApJ*, 509, 633  
 Baan, W. A. & Klöckner, H.-R. 2006, *A&A*, 449, 559  
 Bottinelli, L., Gougouenheim, L., Le Squeren, A. M., Martin, J. M., & Paturel, G. 1990, *IAU Circ.* 4977  
 Darling, J. & Giovanelli, R. 2002a, *AJ*, 124, 100  
 Darling, J. & Giovanelli, R. 2006, *AJ*, 132, 2596  
 Gallimore, J. F., Baum, S. A., O’Dea, C. P., Brinks, E., & Pedlar, A. 1996, *ApJ*, 462, 740  
 Gao, Y. & Solomon, P. M. 2004a, *ApJS*, 152, 63 (GS04a)  
 Gao, Y. & Solomon, P. M. 2004b, *ApJ*, 606, 271  
 Haschick, A. D. & Baan, W. A. 1985, *Nature*, 314, 144  
 Henkel, C. & Wilson, T. L. 1990, *A&A*, 229, 431  
 Krumholz, M. R. & Thompson, T. A. 2007, *ApJ*, submitted (astro-ph/0704.0792)  
 Lo, K. Y. 2005, *ARA&A*, 43, 625  
 Lockett, P., & Elitzur, M. 2007, *ApJ*, submitted  
 Martin, J. M., Le Squeren, A. M., Bottinelli, L., Gougouenheim, L., & Dennefeld, M. 1988, *A&A*, 201, L13  
 Martin, J. M., Le Squeren, A. M., Bottinelli, L., Gougouenheim, L., & Dennefeld, M. 1989, *A&A*, 208, 39  
 Nguyen-Q-Rieu, Mebold, U., Winnberg, A., Guibert, J., & Booth, R. 1976, *A&A*, 52, 467  
 Norris, R. P., Gardner, F. F., Whiteoak, J. B., Allen, D. A., & Roche, P. F. 1989, *MNRAS*, 237, 673  
 Parra, R., Conway, J. E., Elitzur, M., & Pihlstrom, Y. M. 2005, *A&A*, 443, 383  
 Pihlström, Y. M., Conway, J. E., Booth, R. S., Diamond, P. J., & Polatidis, A. G. 2001, *A&A*, 377, 413  
 Rovilos, E., Diamond, P., Lonsdale, C. J., Lonsdale, C. J., & Smith, H. E. 2003, *MNRAS*, 342, 373  
 Rickard, L. J., Turner, B. E., & Bania, T. M. 1982, *ApJ*, 252, 147  
 Schmelz, J. T., Baan, W. A., Haschick, A. D., & Eder, J. 1986, *AJ*, 92, 1291  
 Schmelz, J. T. & Baan, W. A. 1988, *AJ*, 95, 672  
 Solomon, P. M., Downes, D., Radford, S. J. E., & Barrett, J. W. 1997, *ApJ*, 478, 144  
 Staveley-Smith, L., Norris, R. P., Chapman, J. M., Allen, D. A., Whiteoak, J. B., & Roy, A. L. 1992, *MNRAS*, 258, 725  
 Unger, S. W., Chapman, J. M., Cohen, R. J., Hawarden, T. G., & Mountain, C. M. 1986, *MNRAS*, 220, 1P  
 Vignali, C., Brandt, W. N., Comastri, A., & Darling, J. 2005, *MNRAS*, 364, 99  
 Whiteoak, J. B. & Gardner, F. F. 1973, *Astrophys. Lett.*, 15, 211

TABLE 1  
OH PROPERTIES OF HCN-DETECTED GALAXIES

IRAS Name	Other Name	$D_L$ (Mpc)	$L_{IR}$ ( $10^{10} L_{\odot}$ )	$L_{CO}$ ( $10^8$ K km s $^{-1}$ pc $^2$ )	$L_{HCN}$ ( $10^8$ K km s $^{-1}$ pc $^2$ )	OH Type <sup>a</sup>	log $L_{OH}$ ( $L_{\odot}$ )	Ref
00450–2533	NGC253	2.5	2.1	4.6	0.27	abs+kilo	(–1.3)	1
01053–1746	IC1623	81.7	46.7	130.5	8.5	non	...	2
01219+0331	NGC520	31.1	8.5	16.3	0.64	abs+kilo	(–0.4)	3
01403+1323	NGC660	14.0	3.7	7.3	>0.26	abs	...	4
02071+3857	NGC828	75.4	22.4	58.5	1.3	non	...	2
02193+4207	NGC891	10.3	2.6	11.0	0.25	non	...	2
02360–0653	NGC1022	21.1	2.6	4.2	0.20	non	...	2
02391+0013	NGC1055	14.8	2.1	13.3	<0.37	non	...	5
02401–0013	NGC1068	16.7	28.3	20.7	3.61	kilo	(–0.3)	6
02526–0023	NGC1144	117.3	25.1	108.9	2.67	non	...	2
03317–3618	NGC1365	20.8	12.9	58.7	3.10	non*	...	7
03419+6756	IC342	3.7	1.4	9.5	0.47	non	...	2
04315–0840	NGC1614	63.2	38.6	24.5	1.25	non	...	2
05083+7936	VII Zw31	223.4	87.1	125.0	9.8	non	...	2
05189–2524	...	170.3	118.1	67.0	6.2	non*	...	7
06106+7822	NGC2146	15.2	10.0	12.5	0.96	non	...	2
07101+8550	NGC2276	35.5	6.2	10.2	0.40	non	...	2
09126+4432	Arp55	162.7	45.7	125.0	3.8	non	...	2
09293+2143	NGC2903	6.2	0.83	2.3	>0.09	non	...	2
09320+6134	UGC05101	160.2	89.2	50.8	10.0	OHM	1.61	8
09517+6954	M82	3.4	4.6	5.7	0.30	abs+kilo	(–1.7)	9
09585+5555	NGC3079	16.2	4.3	24.0	~1.0	abs	...	10
10566+2448	...	173.3	93.8	61.5	10.2	non	...	2
11010+4107	Arp148	143.3	36.5	>47.0	4.0	OHM	1.98	11
11085+5556	NGC3556	10.6	1.35	>4.5	>0.09	non	...	2
11176+1315	NGC3627	7.6	1.26	4.4	>0.08	non	...	12
11176+1351	NGC3628	7.6	1.01	7.1	0.24	abs	...	4
11257+5850	Arp299	43.0	62.8	29.0	2.1	OHM	1.38	13
11460+4859	NGC3893	13.9	1.15	4.1	0.23	non	...	2
11578–0049	NGC4030	17.1	2.14	15.2	0.54	non*	...	2
11596+6224	NGC4041	18.0	1.70	3.9	0.18	non	...	2
12239+3129	NGC4414	9.3	0.81	4.6	0.16	non	...	5
12396+3249	NGC4631	8.1	2.0	2.3	~0.08	non	...	5
12540+5708	Mrk231	170.3	303.5	82.2	18.6	OHM	2.87	14
12542+2157	NGC4826	4.7	0.26	1.3	>0.04	non	...	12
13025–4911	NGC4945	3.7	2.6	5.8	~0.27	abs	...	1
13086+3719	NGC5005	14.0	1.4	8.2	0.41	non*	...	2
13135+4217	NGC5055	7.3	1.1	8.6	>0.10	non	...	2
13183+3423	Arp193	92.7	37.3	39.8	9.5	abs	...	5
13229–2934	NGC5135	51.7	13.8	31.3	2.73	non*	...	7
...	M51	9.6	4.2	19.4	0.50	non	...	2
13341–2936	M83	3.7	1.4	8.1	0.35	non*	...	15
13428+5608	Mrk273	152.2	129.9	65.0	15.2	OHM	2.53	14
14306+5808	NGC5678	27.8	3.0	17.2	0.75	non	...	2
14376–0004	NGC5713	24.0	4.2	8.1	0.22	non	...	2
14514+0344	NGC5775	21.3	3.8	10.9	0.57	abs*	...	5
15327+2340	Arp220	74.7	140.2	78.5	9.2	OHM	2.58	13
16504+0228	NGC6240	98.1	61.2	79.0	11.0	abs	...	3
17208–0014	...	173.1	234.5	146.9	37.6	OHM	3.02	16
18293–3413	...	72.1	53.7	85.5	4.03	non	...	7
18425+6036	NGC6701	56.8	11.2	34.0	1.38	abs	...	17
...	NGC6921	60.3	11.4	17.5	~2.81	non	...	5
20338+5958	NGC6946	5.5	1.6	9.2	0.49	non	...	2
21453–3511	NGC7130	65.0	21.4	44.9	3.27	non	...	18
22132–3705	IC5179	46.2	14.1	~26.4	3.42	non*	...	7
22347+3409	NGC7331	15.0	3.5	>10.7	>0.44	non	...	2
23007+0836	NGC7469	67.5	40.7	37.1	2.19	abs*	...	5 <sup>b</sup>
23024+1203	NGC7479	35.2	7.4	26.7	1.12	non	...	5
23365+3604	...	266.1	142.0	85.0	15.0	OHM	2.45	19
23488+1949	NGC7771	60.4	21.4	90.8	6.5	non	...	5
23488+2018	Mrk331	75.3	26.9	52.1	3.35	non	...	2

REFERENCES. — (1) Whiteoak & Gardner (1973); (2) Baan *et al.* (1992); (3) Baan *et al.* (1985a); (4) Rickard *et al.* (1982); (5) Schmelz *et al.* (1986); (6) Gallimore *et al.* (1996); (7) Norris *et al.* (1989); (8) Henkel & Wilson (1990); (9) Nguyen-Q-Rieu *et al.* (1976); (10) Haschick & Baan (1985); (11) Martin *et al.* (1988); (12) Schmelz & Baan (1988); (13) Baan *et al.* (1989); (14) Baan *et al.* (1985b); (15) Unger *et al.* (1986); (16) Martin *et al.* (1989); (17) Baan (1989); (18) Staveley-Smith *et al.* (1992); (19) Bottinelli *et al.* (1990).

NOTE. — Columns 2–6 are from Table 1 of Gao & Solomon (2004b). References refer to the OH type and luminosity. Estimates of the emission line luminosity of OH kilomaser, corrected for  $D_L$  listed in Col. 3 and absorption, are listed in Column 8 in parentheses.

<sup>a</sup> OH types refer to: “abs+kilo” for OH absorption and kilomaser emission; “kilo” for OH kilomaser emission; “abs” for OH absorption; “non” for no OH lines detected; and “OHM” for OH megamasers emission. An asterisk (\*) indicates that OH non-detections have a large rms noise level compared to the typical peak maser line, or that the detection of absorption is marginal ( $3\sigma$ ). These objects are not plotted in Figures 1–3 or used for statistics in the text.

<sup>b</sup> NGC 7469 is listed by Baan *et al.* (1992) as a non-detection, but Schmelz *et al.* (1986) claims a  $3\sigma$  detection of OH absorption in a spectrum with an rms noise 3 times smaller than Baan *et al.* (1992).

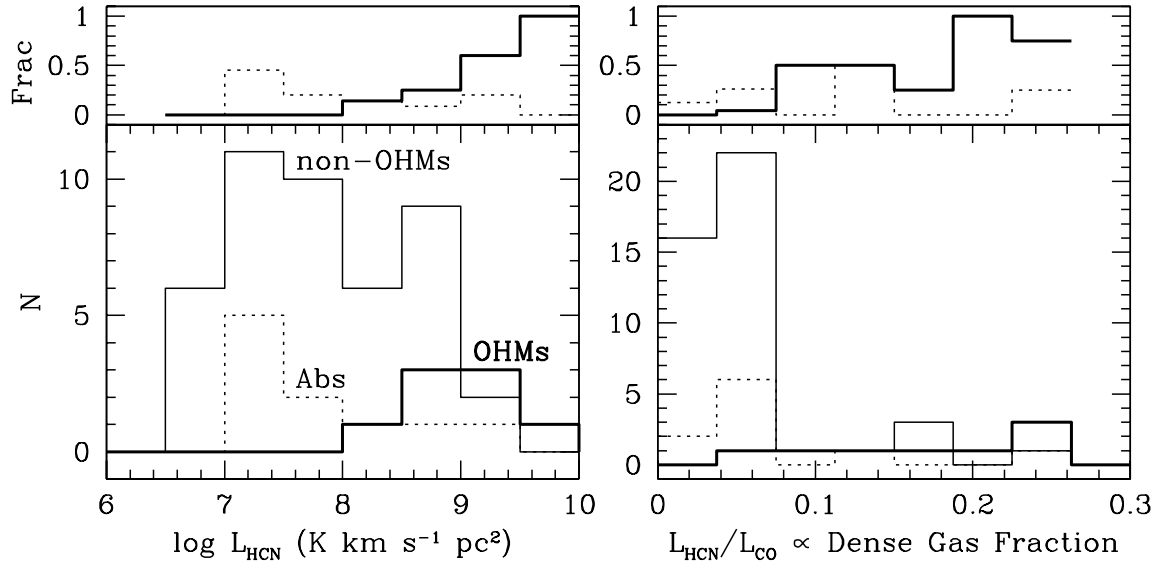


FIG. 3.— Number and fraction of OH megamasers, OH absorbers, and non-OHMs (including absorbers) versus  $L_{\text{HCN}}$  and  $L_{\text{HCN}}/L_{\text{CO}}$ , a proxy for dense gas fraction. The bold line indicates the OHMs, the solid line indicates the non-OHMs, and the dotted line shows the OH absorbers, as indicated in the left panel. The upper panels indicate the fraction of the total sample that shows either OH absorption or emission.